



Antidiabetic activity of green synthesis silver nanoparticles using *Lonicera japonica* leaves extract

Journal:	<i>RSC Advances</i>
Manuscript ID	RA-ART-11-2015-024391.R1
Article Type:	Paper
Date Submitted by the Author:	06-Apr-2016
Complete List of Authors:	Balan, Kannan; Henan University Qing, Weixia ; Henan University, College of Chemistry and Chemical Engineering Wang, You you; Henan University, College of Chemistry and Chemical Engineering Liu, Xiuhua; Henan University, College of Chemistry and Chemical Engineering Thayumanavan, Palvannan; Periyar University, Biochemistry Wang, Yong; Henan University, College of Chemistry and Chemical Engineering Ma, Fanyi; Henan University, College of Chemistry and Chemical Engineering Zhang, Yan; Henan University, College of Chemistry and Chemical Engineering
Subject area & keyword:	Nanomedicine < Nanoscience

Antidiabetic activity of green synthesis silver nanoparticles using

Lonicera japonica leaves extract

Kannan Balan^{a,b}, Weixia Qing^a, Youyou Wang^a, Xiuhua Liu^{a*}, Thayumanavan Palvannan^b, Yong Wang^a, Fanyi Ma^a, Yun Zhang^a

^a*College of Chemistry and Chemical Engineering, Key Laboratory of Natural Medicine and Immune Engineering, Henan University, Kaifeng, Henan Province 475004, P.R. China.*

^b*Department of Biochemistry, Laboratory of Bioprocess and Engineering, Periyar University, Salem, Tamil Nadu 636011, India.*

***Corresponding Author**

Prof. Xiuhua Liu,

Institute of Environmental and Analytical Sciences,

College of chemistry and chemical engineering,

Henan University, Kaifeng-475004,

China.

Email: 11514524@163.com; liuxiuhua@henu.edu.cn

Telephone: +86-371-22199505.

ABSTRACT

In this work we report the green synthesis of silver nanoparticles (AgNPs) using aqueous leaves extract of *Lonicera japonica*. The color change from pale yellow to brown color was observed during synthesis process. Ultraviolet-visible (UV-vis) studies show an absorption band at 435 nm due to surface plasmon resonance of the AgNPs, further characterized using average size and stability of AgNPs were 53 nm and -35.6 mv as determined by zeta sizer. The spherical, hexagonal shape and face centered cubic crystalline structure of metallic silver were confirmed by high resolution transmission electron microscopy (HR-TEM) and X ray diffraction (XRD). The functional group of biomolecules present in the AgNPs was characterized by Fourier transformed infrared spectra (FTIR). The synthesized AgNPs exhibited strong antioxidant activity. The antidiabetic ability of AgNPs showed effective inhibition against carbohydrate digestive enzyme such as α -amylase and α -glucosidase with an IC_{50} value of 54.56 and 37.86 $\mu\text{g/mL}$ respectively. The inhibition of kinetic mechanism was analyzed with LB and Dixon plot. AgNPs was identified to be a reversible non competitive inhibitor and K_i values of 25.9 and 24.6 μg for key enzyme of diabetes (α -amylase and α -glucosidase). We conclude the results suggest that the AgNPs were found to be amazingly potential antidiabetic activity against key enzyme of diabetes and appropriate nanomedicine for nanobiomedical application.

Keywords: AgNPs, Enzyme inhibition, Kinetic profile, *Lonicera japonica*

1. Introduction

Nanomedicine has become a leading research field. Scientists square measured concerned in synthesizing safe, effective, and most of all cheaper and less toxic drugs to combat diseases like diabetes, cancer, epilepsy, etc. These nanoparticles have a site specific action attributable to which only a secure and a prescribed dosage of drug molecules have to be compelled to be administered and therefore helps in reducing the undesired toxicity. These nanoparticles due to their targeted action increase the efficacy of the drug. Their small size gives them an edge where as evading the immune responses and also gives them the ability to cross relatively impermeable membranes¹.

Green synthesis of nanoparticles was more preferred than chemical synthesis since it is involved in the reduction of metals using various hazardous chemicals. Naturally, plants possess both the primary and secondary metabolites to carry out the green synthesis. The green synthesized silver nanoparticles were widely used for many applications such as antidiabetic², antimicrobial³, antioxidant⁴, anticancer⁵ and also used in industries.

Lonicera japonica Thunb (Caprifoliaceae), could be a traditional medicine distributed most over the china. The plant has been reported for its medicinal property such as antiviral⁶, anti-inflammatory⁷ and antibacterial⁸. A various number of compounds have been isolated from these plant phenols⁹, saponins¹⁰, flavonoids¹¹ and polysaccharide¹². The present study deals with the synthesis and characterization of AgNPs using aqueous leaves extract of *L. japonica* and their antidiabetic activity. The antidiabetic targets such as, α -amylase, α -glucosidase and free radical inhibition were used as a model for the present study.

2. Materials and methods

2.1. Chemicals

α -amylase, α -glucosidase, DPPH, p-nitrophenyl- α -D-glucopyranoside (PNPG) and silver nitrate were purchased from Sigma–Aldrich, USA, and all other chemicals were commercial reagent grade.

2.2. Green synthesis of silver nanoparticles using *L. japonica* leaves extract

L. japonica was collected from the Henan University campus, Kaifeng, China during April. AgNPs was synthesized by the method of Parashar et al., (2009)¹⁴ with slight modification. *L. japonica* leaves were washed thoroughly in tap water for 10 minutes in order to get rid of the dirt particles and rinsed briefly in deionized water. The plant leaves broth solution was prepared by taking 10 g of washed and finely cut leaves in a 250 mL erlenmeyer flask besides 100 mL of deionized water and then boiling the mixture at 60 °C for 5 minutes. After boiling, the solution was decanted, and 12 mL of this broth was added to 88ml of 1 mM aqueous AgNO₃ solution and the solution heated at 60 °C for 5 minutes the resulting solution became brown in color. This extract was filtered through nylon mesh, followed by Millipore hydrophilic filter (0.22 μ m) and used for further experiments. A control setup was additionally maintained without *L. japonica* extract and color intensity of the extracts was measured at 435 nm for various time intervals (6, 12, 24, 48 and 72 hrs respectively).

2.3. Characterization of synthesized AgNPs

UV–vis spectroscopic studies were carried out on a Shimadzu UV-1900 spectrophotometer. The average particle size and Zeta potential of the synthesized AgNPs was evaluated with the help of malvern Zeta-sizer Nano ZS90. JEM-2100 high resolution transmission electron microscope was used to study the morphology and size of the

nanoparticles. AgNPs was examined by X-ray diffraction analysis using Bruker D8 Advance, an analytical X-ray diffractometer with a Cu K α radiation monochromatic filter in the range 30–90°. FTIR spectra were recorded on a VERTEX 70 spectrometer using pressed KBr pellets.

2.4. DPPH radical-scavenging activity

The radical scavenging activity of the AgNPs was measured in terms of hydrogen donating or radical-scavenging ability using the stable radical DPPH¹⁵. Solution of DPPH in ethanol (0.1 mM) was prepared and 1.0 mL of this solution was added to 2.0 mL of AgNPs solution at different concentrations (20–100 μ g/mL). Thirty minutes later, the absorbance was measured at 517 nm. Ascorbic acid was used as the positive control. Lower absorbance of the reaction mixture indicated higher radical scavenging activity. Radical scavenging activity was expressed as the inhibition percentage of free radical by the sample and was calculated using the subsequent formula:

$$D = \frac{(A_{ini} - A_{obs})}{A_{ini}} \times 100$$

Where A_{ini} was the absorbance of the control (blank, without AgNPs) and A_{obs} was the absorbance in the presence of the AgNPs.

2.5. α -amylase inhibition assay

The inhibition assay was performed using the DNSA method¹⁶. The assay mixture consisted of 500 μ L of 0.02 M sodium phosphate buffer (containing 6mM NaCl, pH6.9,) containing α -amylase solution (1 U/mL) and AgNPs at a concentration of 20-100 μ g/mL. The assay mixture was preincubated at 37 °C for 20 minutes. After incubation, 250 μ L of 1 % starch solution in the aforementioned buffer was added to the tubes and incubated for 15 minutes at 37 °C. The reaction was terminated by adding 1 mL of dinitrosalicylic acid reagent and then incubated in a boiling water bath for 10 minutes. The tubes were cooled and the absorbance was measured at

540 nm. The reference sample included all other reagents and the enzyme with the exception of the test sample. The α -amylase inhibitory activity was expressed as percentage inhibition. The α -amylase inhibitory activity was calculated according to the equation below:

$$\% \text{ inhibition} = [(A_{i540} - A_{e540}) / A_{i540} \times 100]$$

Where A_{i540} = absorbance without AgNPs; A_{e540} = absorbance with AgNPs.

2.6. α -Glucosidase inhibition activity

The α -glucosidase inhibition was determined by a modified method of from Kim et al., 2005¹⁷. The assay mixture consisted of 150 μ L of 0.1 M sodium phosphate buffer (containing 6 mM NaCl, pH 6.9), 0.1 unit of α -glucosidase, and AgNPs at a concentration of 20-100 μ g/mL. The assay mixture was preincubated at 37 °C for 10 minutes. After incubation, 50 μ L of 2mM paranitrophenyl α -D-glucopyranoside in 0.1 M sodium phosphate buffer was added to the mixture and incubated at 37 °C for 20 minutes. The reaction was terminated by adding 50 μ L of 0.1 M sodium carbonate (Na_2CO_3). The absorbance was measured at 405 nm. The tube with α -glucosidase but without AgNPs served as the control with 100% enzyme activity, and acarbose served as the positive control.

$$\% = (A_{i405} - A_{e405}) / A_{i405} \times 100$$

Where A_{i405} = absorbance without nanoparticles; A_{e405} = absorbance with nanoparticles.

2.7. Inhibitory kinetic analysis

To describe the noncompetitive inhibition mechanism, the Lineweaver–Burk equation in double reciprocal form was expressed as follows:

$$\frac{1}{v} = \frac{K_m}{V_{max}} \left[1 + \frac{I}{K_i} \right] \frac{1}{[S]} + \frac{1}{V_{max}} \left[1 + \frac{[I]}{\alpha K_i} \right] \quad \longrightarrow \quad (1)$$

and secondary plot was constructed as

$$\text{Slope} = \frac{K_m}{V_{max}} + \frac{K_m [I]}{V_{max} K_i} \longrightarrow (2)$$

and

$$Y - \text{Intercept} = \frac{1}{V_{appmax}} = \frac{1}{V_{max}} + \frac{1}{\alpha K_i V_{max}} \longrightarrow (3)$$

where V is the enzyme reaction rate in the absence and presence of AgNPs. K_i and K_m are the inhibition constant and Michaelis–Menten constant, respectively. α is the ratio of the uncompetitive inhibition constant to competitive inhibition constant and the value of α is 1 as a noncompetitive inhibition. $[I]$ and $[S]$ are the concentrations of inhibitor and substrate, respectively. The secondary plots of slope vs. $[I]$ are linearly fitted, assuming a single inhibition site¹⁸.

3. Results and discussion

Initially the synthesized nanoparticles were confirmed by observing, the solution was color changed from pale yellow to brown color. The color change in the reaction mixture indicated the formation of AgNPs¹⁹. During the visual observation, *L. japonica* was mixed with silver nitrate showed a color change from pale yellow to brown due to the reduction of silver ion; which is indicated the formation of AgNPs. (scheme 1). This color arises due to excitation of surface plasmon vibrations in AgNPs^{20,21}. They are the surface active molecules that play an awfully necessary role in reducing and stabilizing process of AgNPs²².

3.1. Characterization of AgNPs

The preliminary characterization of AgNPs was monitored by UV–vis absorbance spectra analysis. The maximum absorbance sturdy peak appears at 435 nm throughout completely

different time intervals of AgNPs by using the *L. japonica* leaves extract (Fig. 1a). The surface plasmon resonance band at 435 nm has confirmed the synthesis of AgNPs at *L. japonica* leaves extract²³. The formation of AgNPs was observed which is established in the absorbance intensity. The DLS size and zeta potential of the synthesized AgNPs is illustrated in Fig. 1 b and c. From the results, the average size of the AgNPs is around 53 nm and the corresponding average negative zeta potential value is -35.6 mV with high colloidal stability. From the literature, it is evident that AgNPs having zeta potential will be stable for a long period^{24,25}.

The morphology and size of the particles were determined by HRTEM. Fig. 2 (a-c) showed that the synthesized AgNPs are spherical and hexagonal in shape with particle range in size from 20 to 60 nm with an average particle size of 52 nm. Fig. 2 (d) shows the selected area electron diffraction (SAED) pattern of the green synthesized AgNPs. Two visible diffraction rings can be clearly observed and indexed as face centered cubic (FCC) metallic silver. The strongest pattern (inner ring) shows the characteristic diffraction rings corresponding to the (111) plane. The outer ring is probably going attributed to the (220) reflection²⁶. The crystalline character of biogenic AgNPs was confirmed by XRD diffraction pattern shown in Fig 3a. The five strong Bragg reflections appearing at 2θ values of 38.26° , 44.47° , 64.66° , 74.54° and 81.68° pertain to the (111), (200), (220), (311) and (222) set of lattice planes. The resultant a peak of AgNPs was matched with the JCPDS (Joint committee on powder diffraction standards) file no – 01 – 087 -0717²⁷.

The FTIR spectrum of synthesized AgNPs (Fig. 3b) shows absorption band at 1637 cm^{-1} corresponds to carbonyl linkages. The peaks at 1385 and 1263 cm^{-1} can be attributed to C-O and C-N stretching vibrations respectively. The absorption peak at 1458 cm^{-1} corresponds to =NH stretching frequency. The peak at 2920 cm^{-1} could be assigned to stretching vibrations of

aliphatic C-H groups. The band at 3400 cm^{-1} corresponds to O-H stretching of hydroxyl group or H-bonded alcohols and phenols. This observation may be confirms bonding between AgNPs.

3.2. Antioxidant activity

Antioxidants have been recognized to exhibit protecting functions against oxidative damage and are associated with reduced risk of chronic diseases. Fig.4 (a) shows DPPH free radical scavenging activity of AgNPs at concentration of 20-100 $\mu\text{g/mL}$. When compared to standard (ascorbic acid) and *L. japonica* extract. The IC_{50} values were found to be 46.70, 26.45 and 72.58 $\mu\text{g/mL}$ for AgNPs, ascorbic acid and *L. japonica* respectively. The results showed radical assay of AgNPs enhanced bit by bit in dose dependant manner. This result is in good agreement with the reported DPPH scavenging activity in the literature for the AgNPs²⁸⁻³⁰.

3.3. Inhibition of AgNPs on α -amylase and α -glucosidase

The carbohydrates digestive enzymes are hydrolyzed by pancreatic α -amylase and intestinal α -glucosidase liable for the breakdown of oligosaccharides and disaccharides into monosaccharides suitable for absorption²⁷. The inhibition of these two digestive enzymes is specifically useful for the treatment of non insulin diabetes because it will slow down the release of glucose in the blood³². As shown in Fig 4 (b) and (c) the results indicated that α -amylase and α -glucosidase were significantly inhibited in a concentration dependent manner following incubation with various concentrations of AgNPs. The increasing concentration of AgNPs level, the enzymatic activity level was reduced remarkably. The IC_{50} values of AgNPs on α -amylase (54.56 $\mu\text{g/mL}$) and α -glucosidase (37.86 $\mu\text{g/mL}$) are showed in Table 1, similar to results obtained in previous report^{2,33}. According to numerous *in vivo* studies, inhibition of α -amylase and α -glucosidase is believed to be one of the most effective approaches for diabetes care³⁴⁻³⁷.

3.4. Mode of inhibition

The mode of kinetic inhibition of AgNPs was determined by the LB plot. The plot based on equation (1) was constructed and displayed Fig.5 (a) and (b). The results shows that double reciprocal plots with straight lines were intercepted at a single point in the second quadrant exhibiting. The plots clearly indicated the pattern of non competitive nature of inhibition. A secondary replot of slope versus (AgNPs) yielded a linear curve, and a replot of Y intercept versus (AgNPs) also yielded a linear curve. These results indicated that AgNPs inhibition follows a typical non competitive mechanism with using equation (1-3). Starch and PNPG were used as an activator (substrate) for α -amylase and α -glucosidase to identify the V_{\max} and K_m value by LB plot (Table 1), subsequently inhibitor constant K_i was found by Dixon plot of α -amylase and α -glucosidase as shown in Fig.5 (c) and (d). The K_i value of α -amylase and α -glucosidase were found to be 25.9 and 24.6 μg respectively. This report well suited to the model of scheme 2.

4. Conclusion

In conclusion we have successfully synthesized AgNPs. The AgNPs exhibited potent carbohydrate degrading enzymes inhibitor for further animal studies and clinical methodology. Based on this result, it is suggested the AgNPs should be used as a nano antidiabetic drugs.

Acknowledgement

This work supported by the support plan of science and technology innovation team in universities and colleges in Henan province of china (14IRTSTHN030).

References

- 1 I. F. Uchegbu, A. G. Schatzlein, Nanotechnology in drug delivery. In: Burger's Medicinal Chemistry, Drug Discovery and Development, seventh ed. *Wiley, Hoboken* 2010.

- 2 K. Rajaram, D. C. Aiswarya, P. Sureshkumar, *Mater Lett*, 2015, **138**, 251–254.
- 3 K. E. Bal, Y. Bal, G. Cote, A. Chagnes, *Mater Lett*, 2012, **79**, 238–41.
- 4 S. Velavan, P. Arivoli, K. Mahadevan, *Nanosci Nanotechnol: Int J*, 2012, **2**, 30–5.
- 5 G. Babu, C. Arulvasu, D. Prabhu, R. Jegadeesh, R. Manikandan, *Mater Lett* 2014, **122**, 98–102.
- 6 C. W. Chang, M. T. Lin, S. S. Lee, K. C. S. C. Liou, F. L. Hsu, J. Y. Lin, *Antiviral Res*, 1995, **27**, 367–374.
- 7 Q. Feng, Y. Ren, Y. Wang, H. Y. Ma, J. Xu, C. R. Zhou, *J. Ethnopharmacol*, 2008, **118**, 51–58.
- 8 A. Rahman, S. C. Kang, *Food Chem*, 2009, **116**, 670–675.
- 9 E. J. Lee, J. S. Kim, H. P. Kim, J. H. Lee, S. S. Kang, *Food Chem*, 2010, **120**, 134–139.
- 10 H. Kawai, M. Kuroyanagi, K. Umehara, A. Ueno, M. Satake, *Chem. Pharm. Bull.*, 1988, **36**, 4769–4775.
- 11 N. Kumar, B. Singh, A. P. Gupta, V.K. Kaul, *Tetrahedron*, 2006, **62**, 4317–4322.
- 12 J. Tian, H. Chem, D. Ha, Y. P. Wei, S. Y. Zheng, *Carbohydr. Polym*, 2012, **90**, 1642–1647.
- 13 Vineet Kumar, Sudesh Kumar Yadav. *Int. J. Green Nanotechnol.*, 2011, **3**, 281–291.
- 14 U. K. Parashar, P. S. Saxenaa, A. Srivastava, *Dig. J. Nanomater. Biostruct.* 2009, **4**, 159–166.
- 15 Y. I. Kwon, E. Apostolidis, Y. C. Kim, K. Shetty, *J. Med. Food.* 2007, **10**, 266–275.
- 16 G. L. Miller, *Anal Chem.* 1959, **31**, 426–428.
- 17 Y. M. Kim, Y. K. Jeong, M. H. Wang, W. Y. Lee, H. I. Rhee, *Nutrition.* 2005, **21**, 756–761.
- 18 Y. X. Si, Z. J. Wang, D. Park, H. Y. Chung, S. F. Wang, L. Yan, J. M. Yang, G. Y. Qian, S. J. Yin, Y. D. Park, *Int. J. Biol. Macromol.* 2012, **50**, 257–262.
- 19 S. S. Shankar, A. Rai, B. Ankamwar, A. Singh, A. Ahmad, M. Sastry, *Nat. Mater.* 2004, **3**, 482–488.

- 20 M. R. Donda, K. R. Kudle, J. Alwala, A. Miryala, B. Sreedhar, M. P. P. Rudra, *Int J Curr Sci.* 2013, **7**, E1-8.
- 21 S. Sharma, S. Kumar, B. D. Bulchandani, S. Taneja, S. Banyal, *Int J Biotechnol Bioeng Res.* 2013, **4**, 711-4.
- 22 M. Dubay, S. Bhadauria, B. S. Kushwah, *Dig J Nanomater Biostruct* 2009, **4**, 537-43.
- 23 M. M. Haytham Ibrahim. *J. of Radi Resear and Appli Sci.* 2015, **8**, 265-275.
- 24 T. J. I. Edison, M. G. Sethuraman, *Process Biochem.* 2012, **47**, 1351-1357.
- 25 K. Prabakar, P. Sivalingam, S. Mohamed Rabeek, M. Muthuselvam, N. Devarajan, A. Arjunan, R. Karthick, M. Suresh, J. P. Wembonyama, *Colloids Surf. B*, 2013, **104**, 282–288.
- 26 Q. Bao, D. Zhang, P. Qi, *J. Colloid Interface Sci.* 2011, **360**, 463–470.
- 27 M. Oćwieja, Z. Adamczyk, K. Kubiak, *J Colloid Interface Sci*, 2012, **376**, 1–11.
- 28 N. Jayachandra Reddy, D. Nagoor Vali, M. Rani, S. Sudha Rani. *Mater. Sci. Eng., C* 2014, **34**, 115–122.
- 29 C. Dipankar, S. Murugan, *Colloids Surf. B* 2012, **98**, 112–119.
- 30 R. Mata, Jayachandra Reddy Nakkala, Sudha Rani Sadras, *Colloids Surf. B*, 2015, **128**, 276–286.
- 31 P.M. De Sales, P.M Souza, L.A. Simeoni, D. Silveira, *J. Pharm. Pharm. Sci.*, 2012, **15**, 141–183.
- 32 Anna Podsędek, Iwona Majewska, Małgorzata Redzynia, Dorota Sosnowska, Maria Koziółkiewicz, *J. Agric. Food Chem.* 2014, **62**, 4610–4617.
- 33 K. Sivaranjani, M. Meenakshisundaram, *Int. Res. J. Pharm.* 2013, **4**, 225–229.

- 34 K. Balan, P. Perumal, N. Sundarabalaaji, T. Palvannan, *J. Mol. Struct.*, 2015, **1081**, 62–68.
- 35 H. A. Hamid, M. M. Yusoff, M. Liu, M. R. Karim, *J. funct foods*, 2015, **16**, 74–80.
- 36 A. Yousefia, R. Yousefia, F. Panahib, S. Sarikhanib, A. R. Zolghadrb, A. Bahaoddinic, A. Khalafi-Nezhadb, *International Journal of Biological Macromolecules* 2015, **78**, 46–55.
- 37 K. Balan, P. Ratha, G. Prakash, P. Viswanathamurthi, S. Adisakwattana, T. Palvannan, *Arabian J chem*, **DOI**: <http://dx.doi.org/10.1016/j.arabjc.2014.07.002>. (2015).

Legends of Schemes

Scheme 1. Reaction protocol for the green synthesis of AgNPs.

Scheme 2. Kinetic reaction protocol.

Legends of Figures

Fig. 1. (a) UV-vis absorbance spectra recorded during the formation of biosynthesized AgNPs at different time intervals. (b) Particle size analysis and (c) Zeta potential stability measurements obtained for synthesized AgNPs.

Fig. 2. (a-c) HR-TEM images of green synthesized AgNPs at different shapes, significations and (d) SAED pattern showing the AgNPs are crystalline structure.

Fig. 3. (a) XRD pattern and (b) FT-IR spectrum of pure synthesized AgNPs.

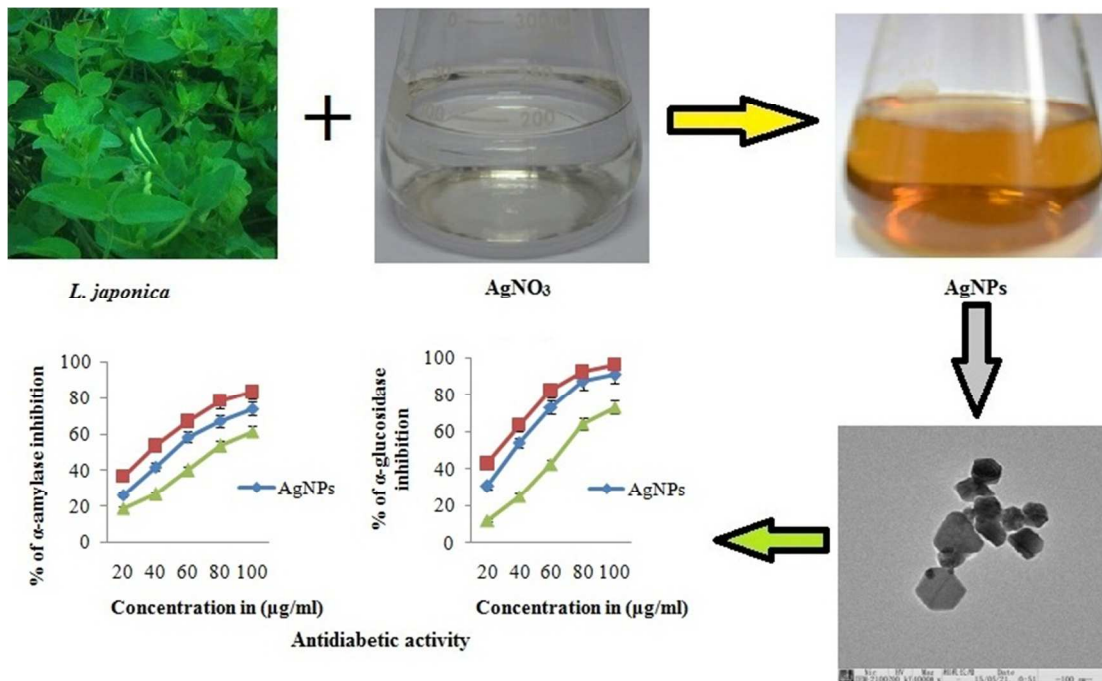
Fig. 4. *In vitro* effect of AgNPs on (a) DPPH scavenging activities, (b) α -amylase and (c) α -glucosidase.

Fig. 5. Lineweaver – Burk plot kinetic analysis the mode of inhibition (a) α -amylase and (b) α -glucosidase inhibitory effects by AgNPs [I]. Dixon plot for determining the kinetic constants for (c) α -amylase and (d) α -glucosidase, substrate [S] were indicated.

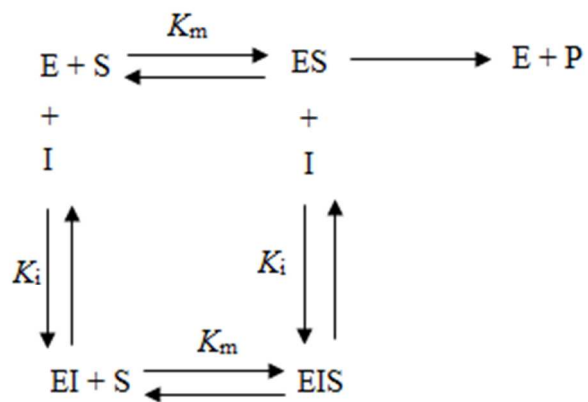
Legends of Table

Table 1

Kinetic properties of AgNPs on α -amylase and α -glucosidase.

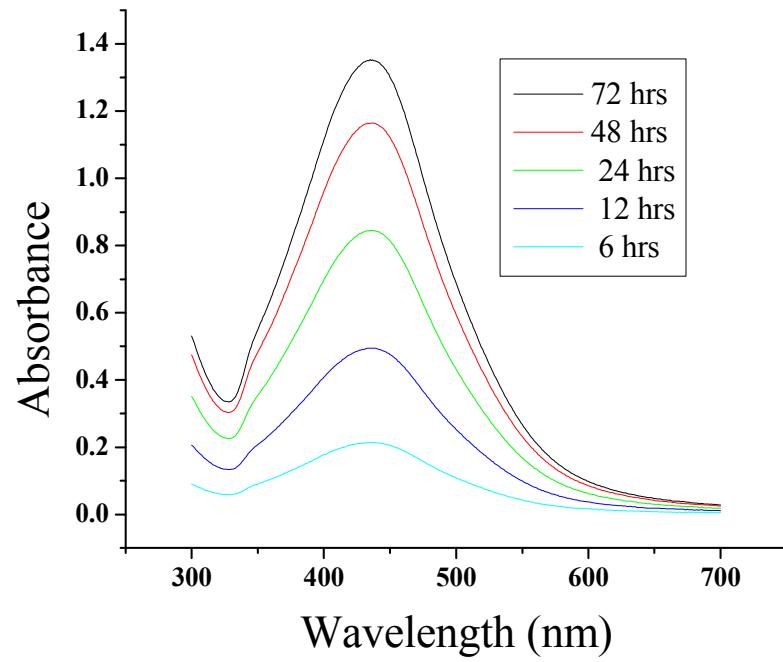


Scheme. 1 Reaction protocol for the green synthesis of AgNPs.

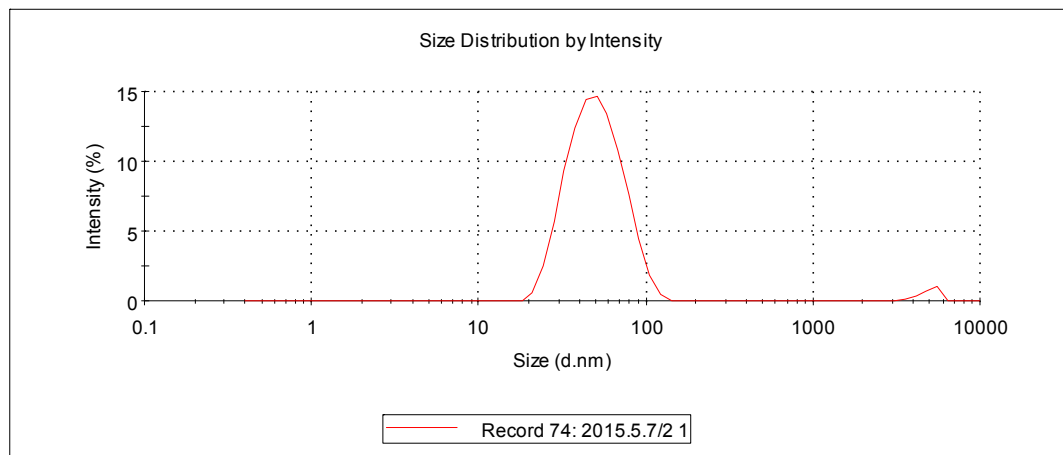


Scheme. 2 Kinetic reaction protocol.

a



b



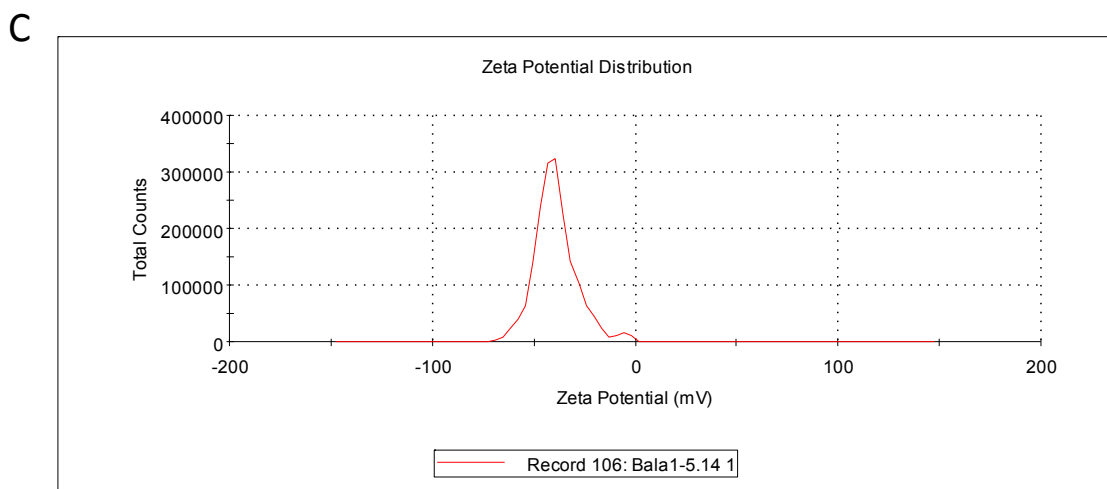
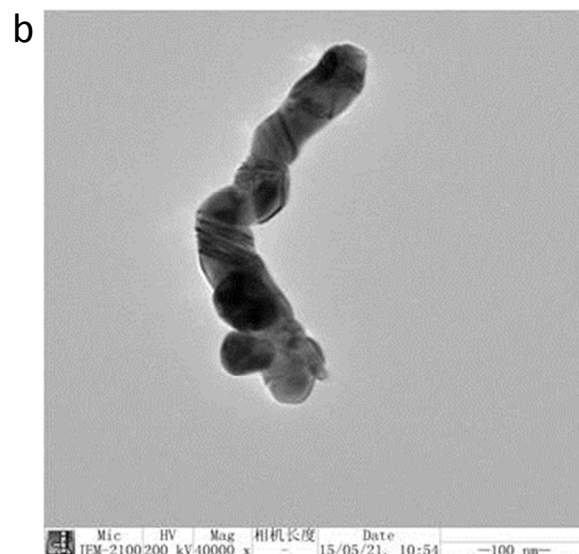
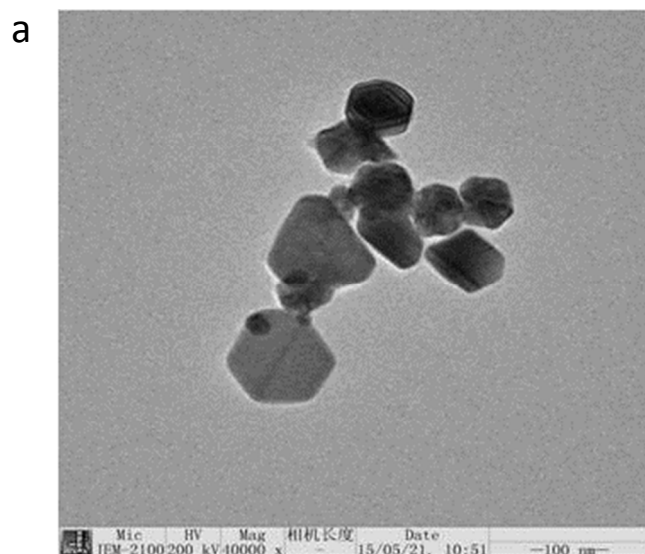


Fig. 1 (a) UV-vis absorbance spectra recorded during the formation of biosynthesized AgNPs at different time intervals. (b) Particle size analysis and (c) Zeta potential stability measurements obtained for synthesized AgNPs.



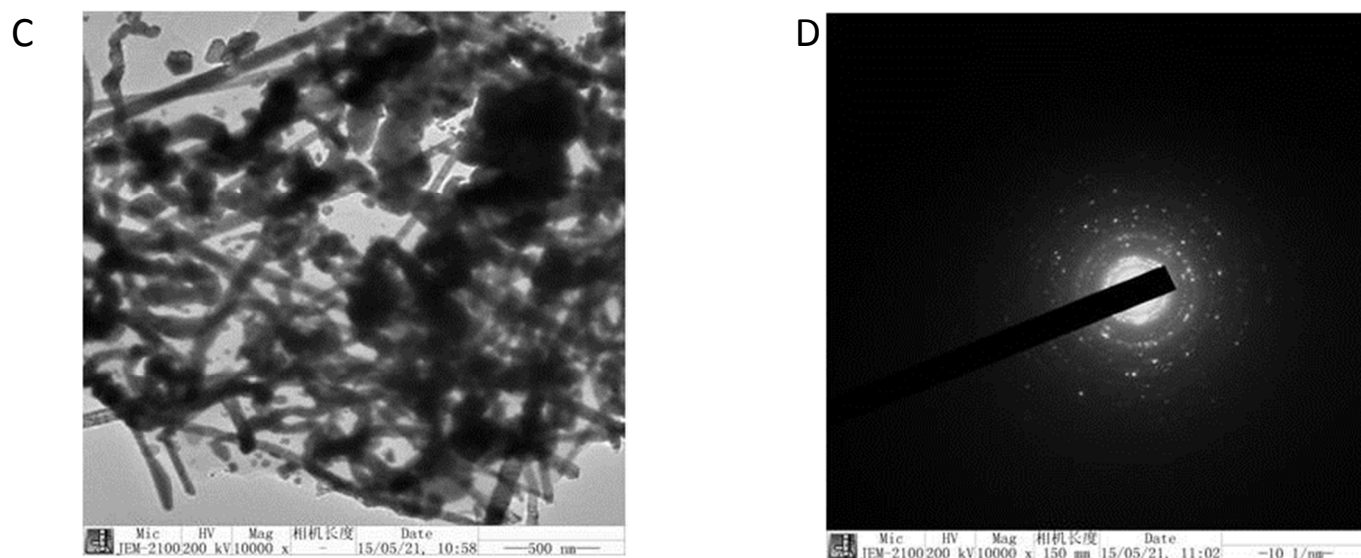
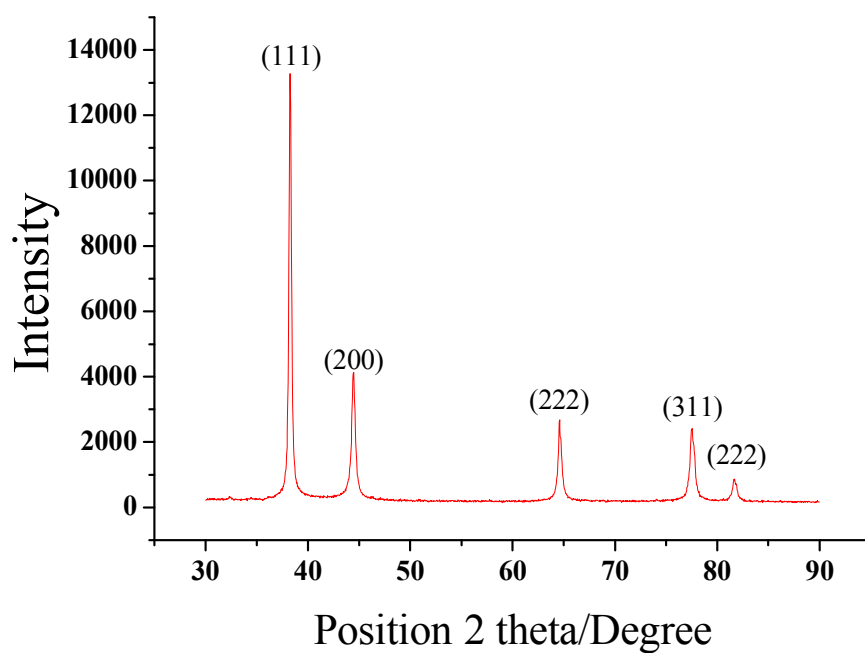


Fig. 2 (a-c) HR-TEM images of green synthesized AgNPs at different shapes, significations and (d) SAED pattern showing the AgNPs are crystalline structure.

a



b

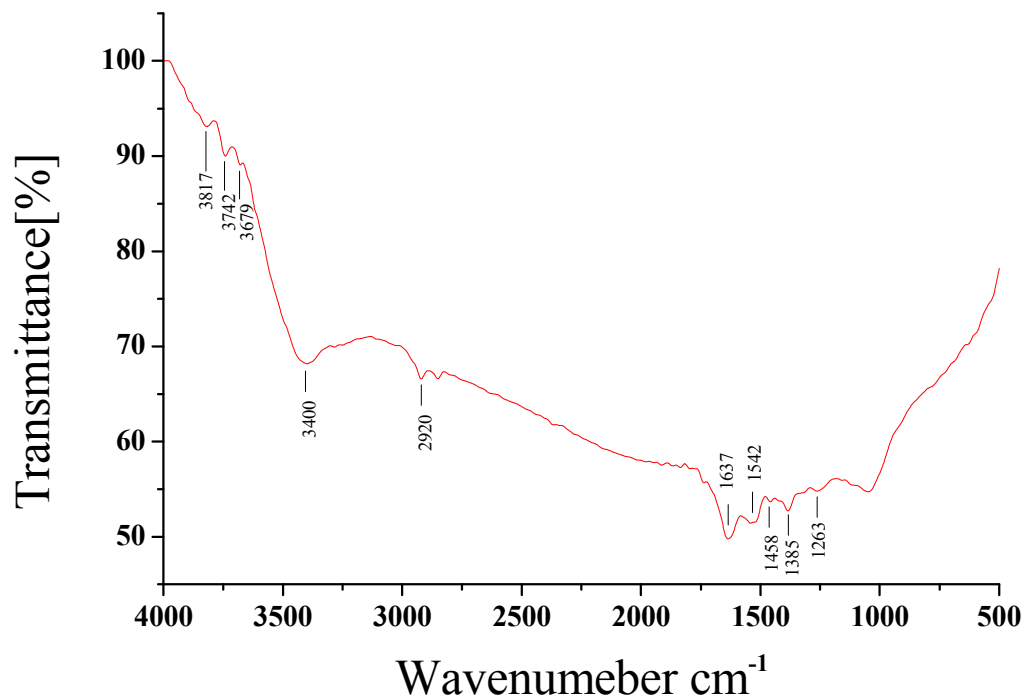
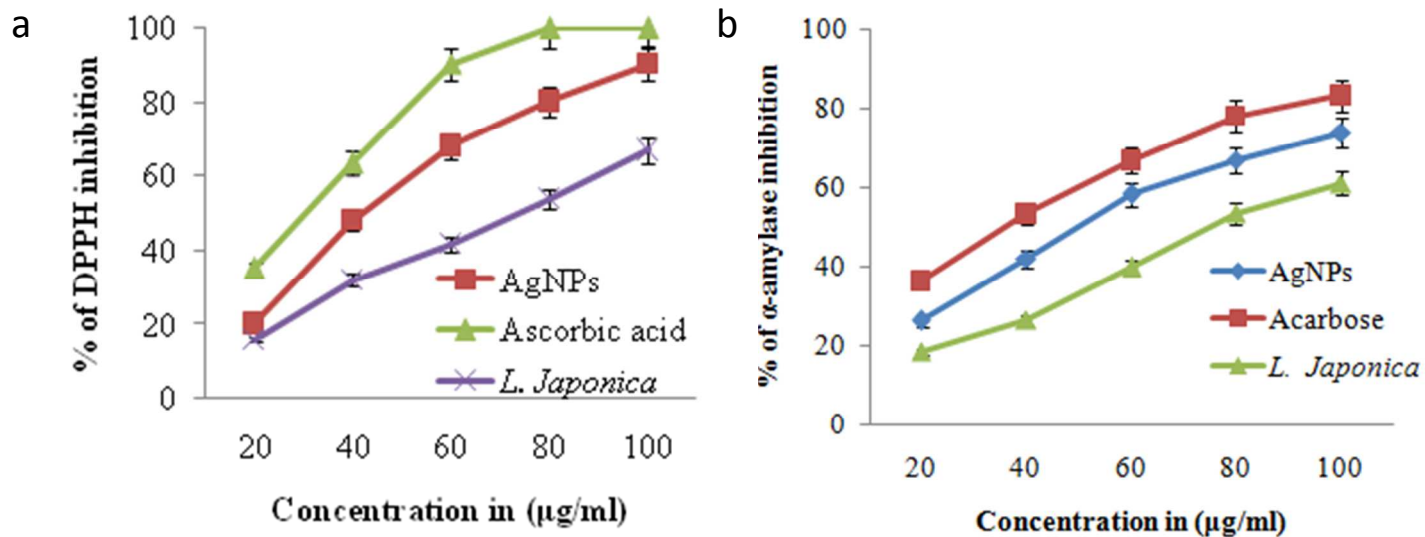


Fig. 3 (a) XRD pattern and (b) FT-IR spectrum of pure synthesized AgNPs.



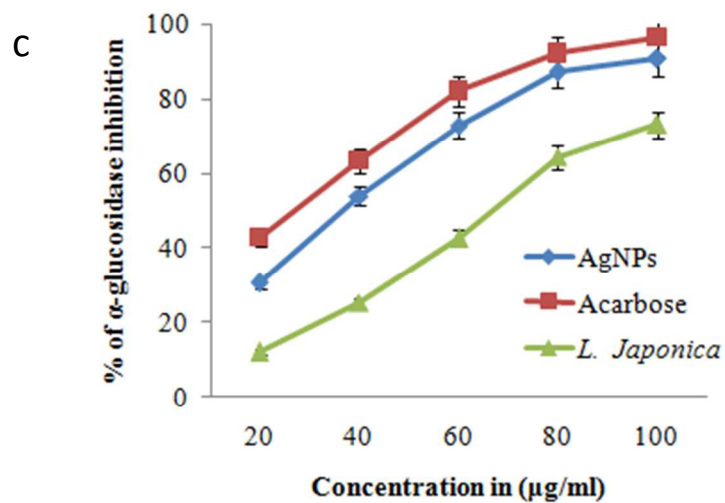
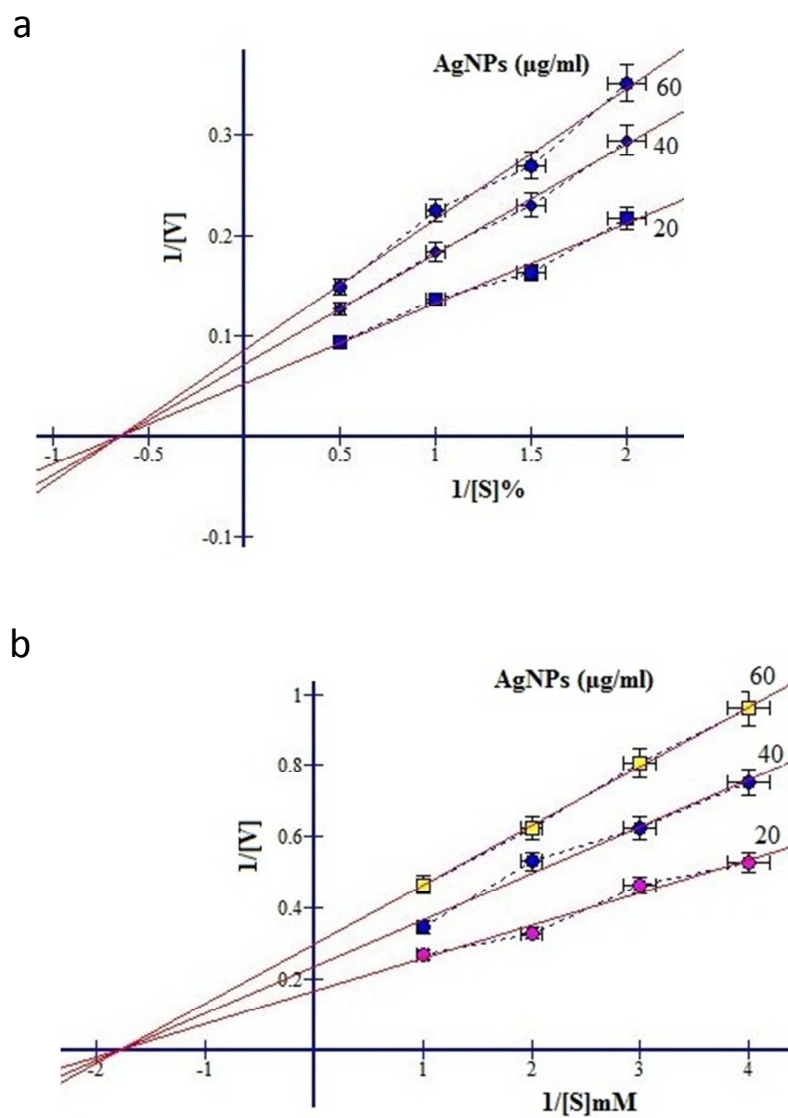
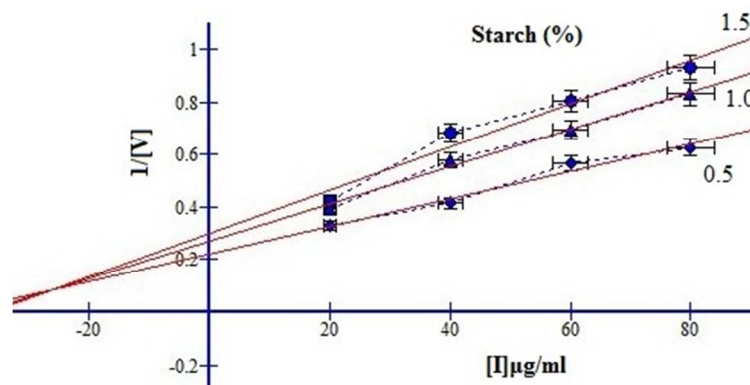


Fig. 4 *In vitro* effect of AgNPs on (a) DPPH scavenging activities, (b) α -amylase and (c) α -glucosidase.



c



d

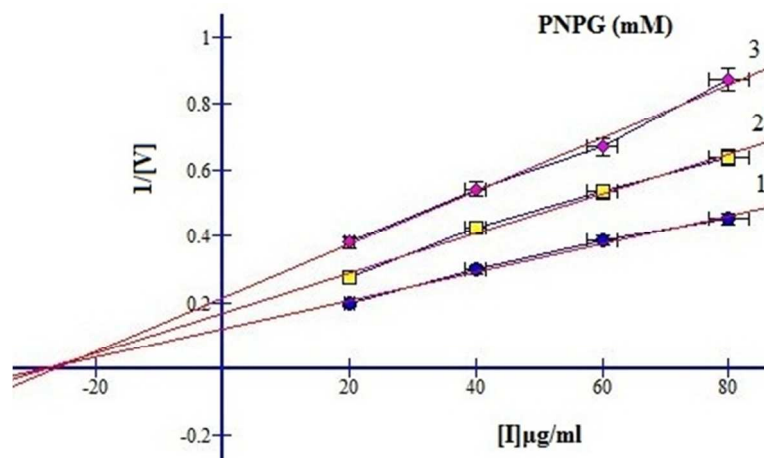


Fig. 5 Lineweaver – Burk plot kinetic analysis the mode of inhibition (a) α -amylase and (b) α -glucosidase inhibitory effects by AgNPs [I]. Dixon plot for determining the kinetic constants for (c) α -amylase and (d) α -glucosidase, substrate [S] were indicated.

Table 1

Kinetic properties of AgNPs on α -amylase and α -glucosidase.

Parameters	α -amylase	α -glucosidase
IC ₅₀	54.56 μ g	37.86 μ g
Mode of inhibition	Noncompetitive	Noncompetitive
K_i	25.9 μ g	24.6 μ g
K_m	0.715%	1.11mM
V_{max}	0.356	0.975

